

Article

Accurate and Efficient Torque Control of an Interior Permanent Magnet Synchronous Motor in Electric Vehicles Based on Hall-Effect Sensors

Lei Yu ¹, Youtong Zhang ^{1,*} and Wenqing Huang ²

¹ Laboratory of Low Emission Vehicle, Beijing Institute of Technology, Beijing 100081, China; yulei0724@bit.edu.cn

² United Automotive Electronic System Co., Ltd., Shanghai 201206, China; hwq086@126.com

* Correspondence: youtong@bit.edu.cn; Tel.: +86-10-6891-5013

Academic Editor: Kuohsiu David Huang

Received: 4 January 2017; Accepted: 14 March 2017; Published: 21 March 2017

Abstract: In this paper, an effective method to achieve accurate and efficient torque control of an interior permanent magnet synchronous motor (IPMSM) in electric vehicles, based on low-resolution Hall-effect sensors, is proposed. The high-resolution rotor position is estimated by a proportional integral (PI) regulator using the deviation between actual output power and reference output power. This method can compensate for the Hall position sensor mounting error, and estimate rotor position continuously and accurately. The permanent magnetic flux linkage is also estimated based on a current PI controller. Other important parameters, such as the d -axis and q -axis inductances, stator resistance, and energy loss, are measured offline by experiments. The measured parameters are saved as lookup tables which cover the entire current operating range at different current levels. Based on these accurate parameters, a maximum torque per ampere (MTPA) control strategy, combined with the feedforward parameter iteration method, can be achieved for accurate and efficient torque control. The effectiveness of the proposed method is verified by both simulation and experimental results.

Keywords: hall-effect sensor; rotor position estimation; interior permanent magnet synchronous motor (IPMSM); torque control; electric vehicle

1. Introduction

The interior permanent magnet synchronous motor (IPMSM) has been widely used in electric vehicles for its high efficiency and high power density. Accurate and efficient torque control is essential for automotive drive systems. However, it is difficult to achieve this target because of the varying parameters of the IPMSM [1].

Although the resolver can obtain high-resolution rotor position of the IPMSM, it is not suitable to be used in vehicles, considering its high cost, weight, and volume. Algorithms based on no position sensors [2] cannot estimate the rotor position accurately in all conditions, in addition to the high-volume computation. In fact, Hall-effect sensors can be used to realize low cost, weight, volume, and high-resolution rotor position. Considering the discrete position signals from Hall-effect sensors, it is quite necessary to conduct research on obtaining continuous rotor position signals.

The most popular method to estimate the rotor position is based on average motor speed [3]. When the motor speed varies frequently, this method may cause a very large error and failure of the control strategy. A vector-tracking observer was proposed to estimate the rotor position in [4]. This method needs to acquire the stator voltages, thus increasing the cost and complexity of the system. An improved vector-tracking observer was proposed to eliminate the complexity of the system in [5]. A method based on back electromotive force (EMF) was proposed in [6]. Although this

method can obtain accurate rotor speed, it cannot obtain accurate rotor position. A method based on flux estimation was proposed for a slotless permanent magnet synchronous motor (PMSM) in [7]. An improved square root unscented Kalman filter (SRUKF) was proposed to estimate rotor speed and position in [8]. Additionally, some studies used linear Hall sensors [9] to estimate rotor position instead of discrete Hall sensors.

To achieve accurate and efficient control, accurate parameters are essential. There are, mainly, two types of methods proposed to achieve parameter identification. One is based on offline measurements, and the other is based on real-time estimating arithmetic [1]. The real-time estimating arithmetic based on the PMSM model was analyzed in [10]. Some parameters must be assumed to be known since not all parameters are identifiable in the steady state. A method was proposed to estimate stator resistance and flux linkage by injecting short-period d -axis current into surface PMSM in [11]. However, it is not suitable for application in vehicles. Mechanical parameters of induction motors were estimated by using voltage sensors only in [12]. The variation of the d -axis and q -axis inductances measured offline [13], or calculated from the finite element [14] in consideration of the cross saturation were proposed. An analytical calculation method of d -axis and q -axis inductances for IPMSM based on winding function theory was proposed in [15]. An adaptive parameter estimator that can achieve maximum torque per ampere (MTPA) control was proposed in [16].

In this paper, an effective method to achieve accurate and efficient torque control of an IPMSM in electric vehicles, based on low-resolution Hall-effect sensors, is proposed. A variety of important parameters are estimated for torque control. To obtain the high-resolution rotor position, an estimation method based on the power closed-loop is proposed with low-resolution Hall-effect sensors. This method can compensate for the Hall position sensor mounting error, and estimate the rotor position continuously and accurately. The permanent magnetic flux linkage is estimated based on a current proportional integral (PI) controller. Other important parameters, such as the d -axis and q -axis inductances, stator resistance, and energy loss are measured offline by experiments. The measured parameters are saved as lookup tables which cover the entire current operating range at different current levels. Combined with the feedforward parameter iteration method, the MTPA control strategy can be achieved based on accurate parameters. As a result, it is an effective approach to realize accurate and efficient torque control.

MATLAB/SIMULINK models were built to analyze the proposed method. Furthermore, experiments were carried out to verify the method.

2. Parameter Estimation

2.1. Analysis of the IPMSM Energy Model

For IPMSM, the input energy comes from the inverter. According to the law of energy conservation, the input energy can be expressed as follows [17]:

$$E_{in} = E_{out} + E_{loss} \quad (1)$$

E_{loss} can be expressed as follows:

$$E_{loss} = E_{Cu} + E_{Fe} + E_{Str} + E_M \quad (2)$$

From the point view of inverter, the input energy can be expressed as follows:

$$E_{in} = \int 3(v_q i_q + v_d i_d) / 2 dt \quad (3)$$

and the output energy can be expressed as follows:

$$E_{out} = \int \omega_e T_e / p dt \quad (4)$$

where ω_e can be obtained from Hall-effect sensors.

Considering the cost, the IPMSM used in vehicles has no torque transducer; hence the actual output energy cannot be obtained from Equation (4). However, if the input energy and the energy loss are known, the output energy can be obtained from Equation (1). The IPMSM energy model can be used to estimate the essential parameters, such as the permanent magnetic flux linkage [18], the difference of the q -axis and d -axis inductance [1]. In this paper, the energy model is used to estimate the high-resolution rotor position based on low-resolution Hall-effect sensors.

2.2. Rotor Position Estimation

2.2.1. Rotor Position Estimation Based on Average Motor Speed

The high-resolution rotor position can easily be estimated through a method based on average rotor speed, where the six sectors are classified according to the states of the Hall sensor's signals [4]. Assuming that the rotor speed within a sector is constant and the average speed in present and previous sectors is uniform, the rotor speed can be approximated as follows [3]:

$$\omega_e = \frac{\theta_1 - \theta_0}{t_1 - t_0} = \frac{d\theta}{t_1 - t_0} \quad (5)$$

where $d\theta$ is the electrical degree between two sectors, $t_1 - t_0$ is the time interval of the previous sector; then the rotor position can be estimated as follows:

$$\theta^* = \theta_1 + \omega_e t = \theta_1 + \frac{d\theta}{t_1 - t_0} t \quad (6)$$

Similarly, the high-resolution rotor position can be obtained, as shown in Figure 1.

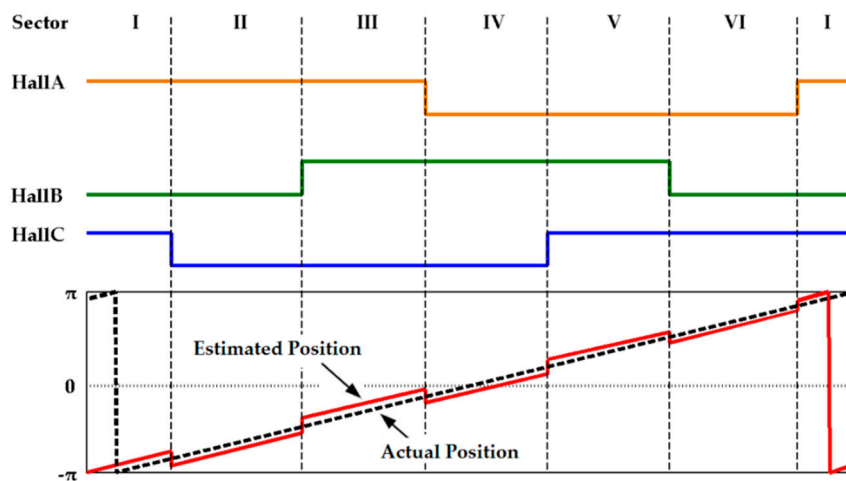


Figure 1. Output signals of the Hall sensors and resultant position estimation.

$\theta_1 - \theta_0$ should be 60 degrees if the Hall sensors are aligned accurately. However, in the IPMSM, there is a certain error in the hall sensor installation. The back EMF can be used to avoid the error and eliminate the third harmonic. However, large estimation errors will occur when this method is used in vehicles where the motor speed changes frequently.

2.2.2. Rotor Position Estimation Based on the Power Closed-Loop Method

For improving the accuracy of estimated rotor position, a method based on the power closed-loop is proposed to estimate the rotor position, as shown in Figure 2.

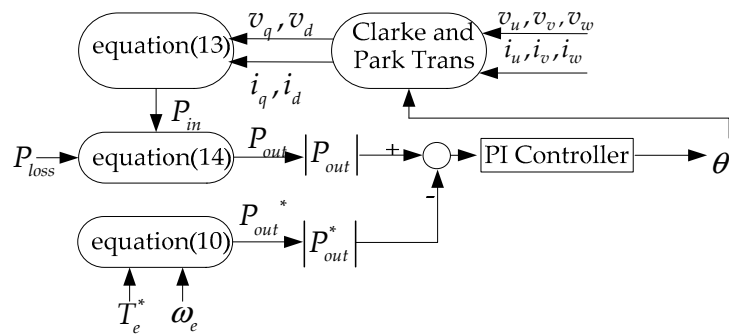


Figure 2. Rotor position estimation based on the power closed-loop method.

The reference electromagnetic torque T_e^* can be expressed as follows:

$$T_e^* = \frac{3}{2}p \left(\hat{\varphi}_f i_{oq}^* - dL i_{od}^* i_{oq}^* \right) \tag{7}$$

where:

$$i_{od}^* = i_d^* - i_{cd} = \frac{1}{A} \left(i_d^* + \frac{\omega_e L_q i_q^*}{R_c} - \frac{\omega_e^2 L_q \varphi_f}{R_c^2} \right) \tag{8}$$

$$i_{oq}^* = i_q^* - i_{cq} = \frac{1}{A} \left(i_q^* - \frac{\omega_e (\varphi_f + L_d i_d^*)}{R_c} \right)$$

$$A = 1 + \frac{\omega_e^2 L_d L_q}{R_c^2} \tag{9}$$

The reference output power can be expressed as follows:

$$P_{out}^* = T_e^* \omega_e / p \tag{10}$$

For the current closed-loop control, the stator d -axis and q -axis current i_d and i_q can be expressed as follows:

$$i_d = i_d^*, i_q = i_q^*, (i_d, i_q) = \text{ParkTrans}(\text{ClarkeTrans}(i_u, i_v, i_w), \theta^*) \tag{11}$$

The output voltage of the d -axis and q -axis can be expressed as follows:

$$(v_d, v_q) = \text{ParkTrans}(\text{ClarkeTrans}(v_u, v_v, v_w), \theta^*) \tag{12}$$

The input power from inverter to motor P_{in} can be expressed as follows:

$$P_{in} = 3(v_q i_q + v_d i_d) / 2 \tag{13}$$

The actual mechanical output power P_{out} can be expressed as follows:

$$P_{out} = P_{in} - P_{loss} \tag{14}$$

Assuming that the estimated rotor position is equal to the actual rotor position, then the actual electromagnetic torque should be equal to the reference electromagnetic torque, and the actual output power should be equal to the reference output power and vice versa. Therefore, the estimated rotor position can be adjusted to realize the equality of the actual output power and the reference output power. To achieve accurate torque control, a PI estimator with robust control is designed to obtain rotor position in this paper.

As shown in Equation (7), the permanent flux linkage and the difference of d -axis and q -axis inductances are used to calculate the reference electromagnetic torque. These parameters influence

the accuracy of rotor position estimation significantly. In this paper, the permanent flux linkage is estimated online and difference of d -axis and q -axis inductances is measured offline by experiments.

2.3. Permanent Magnetic Flux Linkage Estimation

To realize accurate and efficient current control, the current PI controller with feedforward control voltage based on space vector pulse width modulation (SVPWM) is shown in Figure 3 [19].

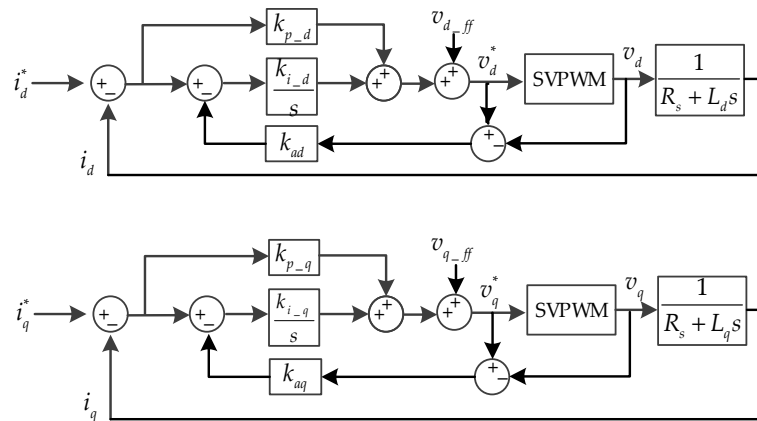


Figure 3. Current proportional integral (PI) controller.

For an IPMSM, it is needed to decouple the d -axis and q -axis voltages and current. The d -axis and q -axis voltages in the rotor rotating coordinate system can be expressed as follows:

$$\begin{bmatrix} v_d \\ v_q \end{bmatrix} = \begin{bmatrix} R_s & 0 \\ 0 & R_s \end{bmatrix} \begin{bmatrix} i_d \\ i_q \end{bmatrix} + \begin{bmatrix} s & 0 \\ 0 & s \end{bmatrix} \begin{bmatrix} \varphi_d \\ \varphi_q \end{bmatrix} + \begin{bmatrix} 0 & -\omega_e \\ \omega_e & 0 \end{bmatrix} \begin{bmatrix} \varphi_d \\ \varphi_q \end{bmatrix} \quad (15)$$

The last term of Equation (15) is the back EMF. If the d -axis and q -axis flux linkages are accurate, it can be eliminated by decoupling control. The feedforward control voltages can be expressed as follows:

$$\begin{bmatrix} v_{d_ff} \\ v_{q_ff} \end{bmatrix} = \begin{bmatrix} 0 & -\omega_e \\ \omega_e & 0 \end{bmatrix} \begin{bmatrix} \hat{\varphi}_d \\ \hat{\varphi}_q \end{bmatrix} \quad (16)$$

where v_{d_ff} and v_{q_ff} are the d -axis and q -axis feedforward control voltages, $\hat{\varphi}_d$ and $\hat{\varphi}_q$ are the estimated d -axis and q -axis flux linkages.

Assuming v_{d_fb} and v_{q_fb} are the outputs of the PI controller, the d -axis and q -axis voltages can be expressed as follows:

$$\begin{bmatrix} v_d \\ v_q \end{bmatrix} = \begin{bmatrix} v_{d_fb} \\ v_{q_fb} \end{bmatrix} + \begin{bmatrix} v_{d_ff} \\ v_{q_ff} \end{bmatrix} \quad (17)$$

In steady circumstance, the actual current follows well to the reference current, and thus the differential term of Equation (15) can be eliminated:

$$\begin{aligned} \begin{bmatrix} v_d \\ v_q \end{bmatrix} &= \begin{bmatrix} R_s & 0 \\ 0 & R_s \end{bmatrix} \begin{bmatrix} i_d \\ i_q \end{bmatrix} + \begin{bmatrix} 0 & -\omega_e \\ \omega_e & 0 \end{bmatrix} \begin{bmatrix} \varphi_d \\ \varphi_q \end{bmatrix} \\ &= \begin{bmatrix} v_{d_fb} \\ v_{q_fb} \end{bmatrix} + \begin{bmatrix} 0 & -\omega_e \\ \omega_e & 0 \end{bmatrix} \begin{bmatrix} \hat{\varphi}_d \\ \hat{\varphi}_q \end{bmatrix} \end{aligned} \quad (18)$$

Furthermore:

$$\begin{bmatrix} v_{d_fb} \\ v_{q_fb} \end{bmatrix} = \begin{bmatrix} R_s & 0 \\ 0 & R_s \end{bmatrix} \begin{bmatrix} i_d \\ i_q \end{bmatrix} + \begin{bmatrix} 0 & -\omega_e \\ \omega_e & 0 \end{bmatrix} \begin{bmatrix} \varphi_d - \hat{\varphi}_d \\ \varphi_q - \hat{\varphi}_q \end{bmatrix} \quad (19)$$

As shown in Equation (19), the outputs of the current PI controller contain a voltage drop at stator resistance and an error of estimated flux linkage. If the variation of the stator resistance is negligible or can be compensated, the error of the estimated flux linkage can be obtained from the integration term of the PI controller, that is:

$$\begin{bmatrix} \Delta\varphi_d \\ \Delta\varphi_q \end{bmatrix} = \frac{1}{\omega_e} \begin{bmatrix} 0 & 1 \\ -1 & 0 \end{bmatrix} \left(\begin{bmatrix} v_{d_fb_i} \\ v_{q_fb_i} \end{bmatrix} - \begin{bmatrix} R_s & 0 \\ 0 & R_s \end{bmatrix} \begin{bmatrix} i_d \\ i_q \end{bmatrix} \right) \quad (20)$$

where $\Delta\varphi_d$ and $\Delta\varphi_q$ are the errors of d -axis and q -axis flux linkages between actual and estimated value ($\Delta\varphi_d = \varphi_d - \hat{\varphi}_d$, $\Delta\varphi_q = \varphi_q - \hat{\varphi}_q$), $v_{d_fb_i}$ and $v_{q_fb_i}$ are the integration terms of the PI controller.

Then, the estimated permanent magnetic flux linkage can be expressed as follows:

$$\hat{\varphi}_f = \varphi_d + \Delta\varphi_d - L_d i_d = (v_q - R_s i_q) / \omega_e - L_d i_d \quad (21)$$

As shown in Equation (21), the accuracy of the estimated permanent magnetic flux linkage is affected by the q -axis voltage (v_q), the d -axis and q -axis inductances (L_d, L_q), the stator resistance (R_s), and the d -axis and q -axis current (i_d, i_q). v_q is equivalent to the reference voltage, which includes the output lag compensation [20] and dead time compensation [21]. In this paper, L_d, L_q , and R_s are measured offline by experiments. The measured parameters are saved as lookup tables which cover the entire current operating range at different current levels. Thus, L_d, L_q , and R_s can be considered to be accurate. In fact, R_s is approximately accurate with temperature compensation, especially at a high speed when the back EMF is much greater than the voltage drop at stator resistance. i_d, i_q can be obtained from current sensors and Hall-effect sensors. Considering the rotor electrical angular speed (ω_e) is in the denominator, the estimation should be avoided at too low speed.

3. Torque Control Strategy

3.1. Feedforward Parameter Iteration Method

A variety of parameters are needed for obtaining the target current. The rotor position and permanent magnetic flux linkage can be estimated, as mentioned above. Other important parameters, such as the d -axis and q -axis inductances, stator resistance, and energy loss, are measured offline by experiments. The measured parameters are saved as lookup tables which cover the entire current operating range at different current levels. The parameters are obtained according to the present input current, and then the target current is calculated according to control strategies. Therefore, the parameters do not match the target current well [22].

Assuming the responding time from zero to maximum torque T_{emax} is $t_{respond}$, the largest change in value of the electromagnetic torque in a control period can be expressed as follows:

$$T_{e_change} = \frac{T_{emax}}{2t_{respond}f} \quad (22)$$

The largest change in value of the q -axis current in a control period can be expressed as follows:

$$i_{q_change} = \frac{T_{emax}}{3p\varphi_f t_{respond}f} \quad (23)$$

In fact, the torque demand varies frequently for the IPMSM used in vehicles, and the target current is calculated according to the actual torque demand. It is difficult to define an equation to calculate the mismatch between the parameters and current. For a given torque demand, starting with present parameters (the d -axis and q -axis inductances, stator resistance, and energy loss), one set of d -axis and q -axis current is obtained, which is calculated by control strategies (such as MTPA). The obtained current is used for a new set of motor parameter calculation (using parameter lookup tables). Another set of d -axis and q -axis current is calculated with the new parameters. This recursive calculation is carried out until the differences between the new output current and the previous one have reached a defined minimum error [22]. The feedforward parameter iteration method follows five steps:

- (1) Obtain the present motor parameters (the d -axis and q -axis inductances, stator resistance, and energy loss) from lookup tables;
- (2) Calculate one set of d -axis and q -axis current using control strategies;
- (3) Calculate the motor parameters with the current from step 2 using lookup tables;
- (4) Calculate another set of d -axis and q -axis current with the new set of motor parameters from step 3 using control strategies.
- (5) If the current error is within tolerance between the current and the previous step, the iteration is complete. Otherwise, return to step 2.

3.2. Maximum Torque Per Ampere Control Strategy

The MTPA control strategy is an efficiency optimization algorithm which only considers the copper loss. The aim of the optimization algorithm is to realize the minimum copper loss for a given torque. Since the copper loss is proportional to the square of stator current, it is essential to find the minimum stator current for a given torque. The MTPA control strategy can be expressed as follows:

$$\begin{aligned} i_{cd} &= 0 \\ i_{cq} &= 0 \\ i_{od} &= i_d - i_{cd} = i_d \\ i_{oq} &= i_q - i_{cq} = i_q \end{aligned} \quad (24)$$

$$T_e = \frac{3}{2} p (\varphi_f i_q + (L_d - L_q) i_d i_q) \quad (25)$$

$$\min \left\{ P_{Cu} = \frac{3}{2} R_s (i_d^2 + i_q^2) = \frac{3}{2} R_s \left[i_d^2 + \left(\frac{2T_e}{3p(\varphi_f + (L_d - L_q)i_d)} \right)^2 \right] \right\} \quad (26)$$

For an IPMSM, $L_d \neq L_q$, Equation (26) has no explicit solutions for a given torque. If the control parameter is the q -axis current [23] or the amplitude of stator current [24], the explicit solution of i_d can be expressed by i_q as follows:

$$i_d = \frac{\varphi_f - \sqrt{\varphi_f^2 + 4(L_q - L_d)^2 i_q^2}}{2(L_q - L_d)} \quad (27)$$

or the explicit solution of i_d can be expressed by i_s as follows:

$$i_d = \frac{\varphi_f - \sqrt{\varphi_f^2 + 8(L_q - L_d)^2 i_s^2}}{4(L_q - L_d)} \quad (28)$$

normalizing Equation (25), it can be expressed as follows:

$$T_{en} = i_{qn}(1 - i_{dn}) \quad (29)$$

where

$$\begin{aligned} i_b &= \varphi_f / (L_q - L_d), \quad T_{eb} = 1.5p\varphi_f i_b \\ i_{dn} &= i_d / i_b, \quad i_{qn} = i_q / i_b, \quad T_{en} = T_e / T_{eb} \end{aligned} \quad (30)$$

Equation (29) shows that the output torque depends on the d -axis and q -axis current. For a given T_{en} , i_{qn} and i_{dn} have no unique solution. Substituting Equation (29) into Equation (26), the MTPA control strategy can be expressed as follows:

$$\min \left\{ P_{Cu} = \frac{3}{2} R_s i_b^2 \left[i_{dn}^2 + \frac{T_{en}^2}{(1 - i_{dn})^2} \right] \right\} \quad (31)$$

For a given IPMSM, R_s and i_b are certain, and the MTPA control strategy can be expressed as follows:

$$\min \left\{ i_{dn}^2 + \frac{T_{en}^2}{(1 - i_{dn})^2} \right\} \quad (32)$$

solving Equation (32):

$$\begin{aligned} T_{en} &= \sqrt{i_{dn}(i_{dn} - 1)^3} \\ T_{en} &= \frac{i_{qn}}{2} (1 + \sqrt{1 + 4i_{qn}^2}) \end{aligned} \quad (33)$$

Although the relationship between the normalized torque and stator current can be obtained, Equation (33) has no explicit solutions either. However, i_{dn} and i_{qn} can be obtained from the lookup tables, as shown in Figure 4. One of the current can be obtained from the lookup tables. The other current can be obtained from the lookup tables directly or calculated by the first current.

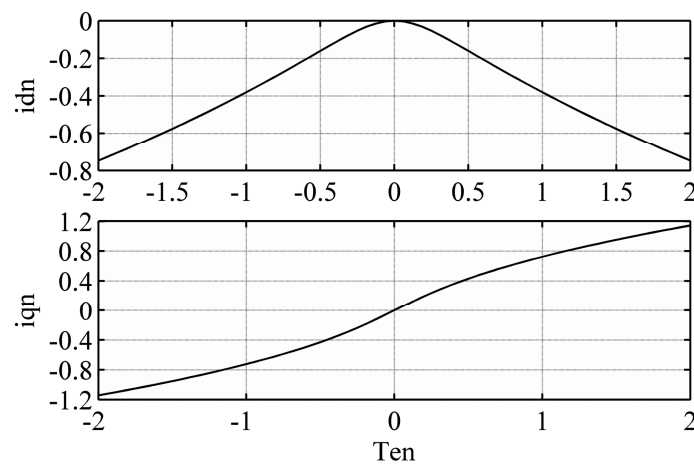


Figure 4. Lookup tables of i_{dn} and i_{qn} to T_{en} .

The MTPA control strategy only needs two lookup tables, which are independent of the motor parameters, hence it is widely used in the IPMSM for its simplicity and small amount of calculations. The IPMSM control system with the MTPA control strategy is shown in Figure 5.

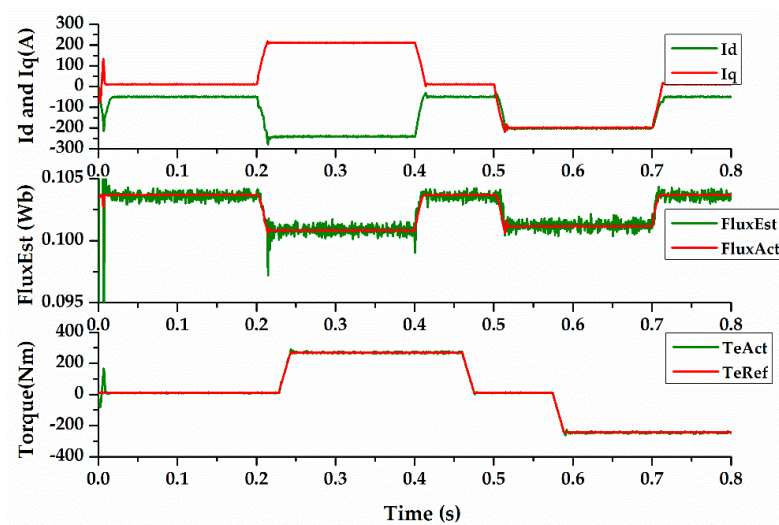


Figure 9. Flux linkage estimation and torque control in the flux weakening region (2800 rpm/256 Nm).

4.2. Experimental Results

The effectiveness of the proposed method was tested experimentally with the IPMSM as Table 1 shows. A dynamometer was used to emulate the load. A digital signal processor (DSP) was used to carry out the real-time algorithm. Six-pack insulated gate bipolar transistors (IGBT) were used as power switches. A LiFePO₄ battery pack (288 V/180 Ah) was used as a power source. The experimental bench is shown in Figure 10.

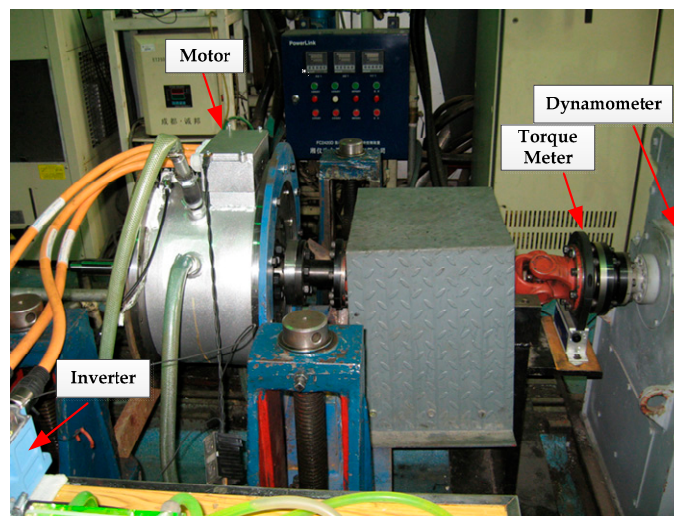


Figure 10. Experimental bench.

The experimental results are shown in Figures 11–13.

As shown in Figures 11 and 12, the minimum rotor position error is less than one electrical degree and the maximum rotor position error is less than five electrical degrees. However, the maximum rotor position error with the average speed based estimation method is around ten electrical degrees [4]. Furthermore, the output torque of motor is always accurate.

Figure 11 shows that the voltage of battery drops dramatically to 250 V under rated conditions, hence, the motor enters the flux-weakening region. Compared with the simulation results, q -axis current decreases, whereas d -axis current increases, and magnetic saturation is not so serious. Thus, the estimated flux linkage in the experiment is slightly greater than the simulation result.

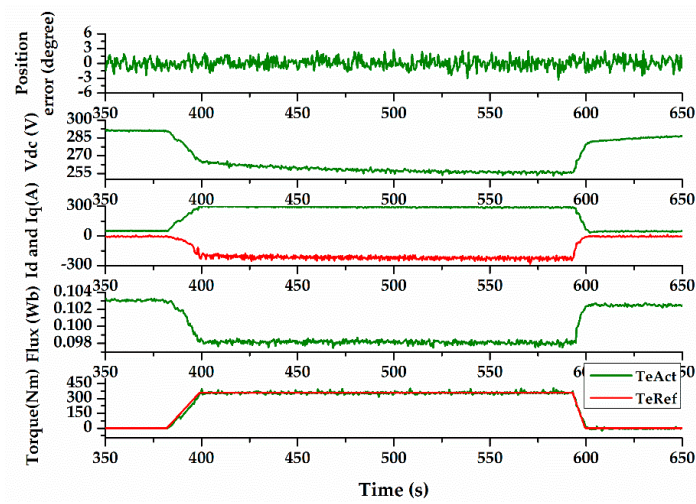


Figure 11. Experimental results under rated conditions (2000 rpm/358 Nm).

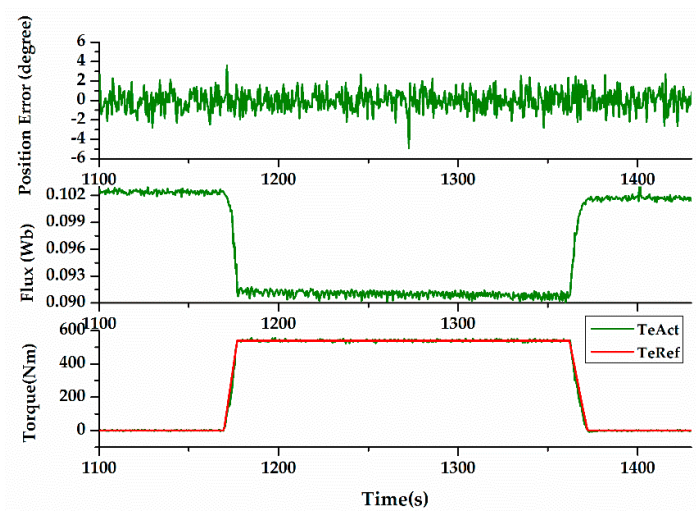


Figure 12. Experimental results under maximum torque conditions (1000 rpm/540 Nm).

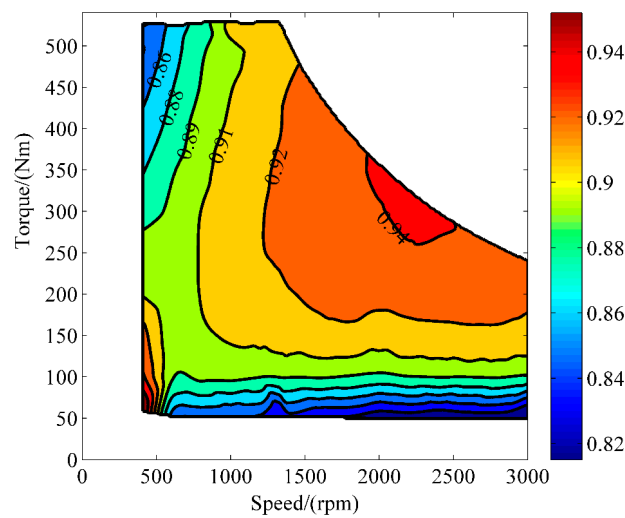


Figure 13. Efficiency of the motor drive system.

Figure 12 shows almost the same results with the simulation except that the flux linkage decreases due to the increment of temperature. Under the maximum torque conditions, the reluctance torque is greater than the other conditions; hence less current is needed to obtain the same output torque. Therefore, the torque control is more efficient.

Figure 13 shows the efficiency of the motor drive system, including the motor and inverter. As shown, the maximum efficiency of the motor drive system can reach 0.94 around the rated conditions, and the minimum efficiency of the system is above 0.8. Thus, the efficient control has been realized.

5. Conclusions

In this paper, an effective method to achieve accurate and efficient torque control of an IPMSM in electric vehicles, based on low-resolution Hall-effect sensors, is proposed. Assuming that the d -axis and q -axis inductances, stator resistance, and energy loss are known (measured offline), the high-resolution rotor position and permanent flux linkage are estimated online based on the IPMSM energy model. Combined with the feedforward parameter iteration method, the MTPA control strategy is achieved based on accurate parameters. The simulation and experimental results show that, by using this method, accurate and efficient torque control can be realized.

By using low-resolution Hall-effect sensors instead of resolvers, electric vehicles can reduce cost, weight, and volume. Since the rotor position estimation is based on a power closed-loop, the IPMSM can output accurate torque even if the estimated rotor position has some errors.

Since the flux linkage and power calculations are related to rotor speed, the proposed method may have some drawbacks in the low-speed region. However, this method provides a relatively more effective way to achieve the efficient and accurate control of IPMSM, particularly when the IPMSM works under high-power, high-speed working conditions. Moreover, the method proposed in this paper can also be applied in other types of motors in electric vehicles, such as in-wheel motors, surface PMSM, and PM-assisted synchronous reluctance motors.

Author Contributions: This paper is the results of the hard work of all of the authors. Lei Yu and Wenqing Huang conceived and designed the proposed method. Lei Yu and Youtong Zhang conceived and performed the experiments; Lei Yu analyzed the data; and Lei Yu wrote the paper. All authors gave advice for the manuscript.

Conflicts of Interest: The authors declare no conflict of interest.

Nomenclature

E_{in}	Input energy
E_{out}	Output energy
E_{loss}	Energy loss
E_{Cu}	Copper loss
E_{Fe}	Iron loss
E_{str}	Stray loss
E_M	Mechanical loss
v_u, v_v, v_w	Stator three phase voltages
v_d, v_q	Stator d -axis and q -axis voltages
v_d^*, v_q^*	Reference stator d -axis and q -axis voltages
i_u, i_v, i_w	Stator three phase current
i_d, i_q	Stator d -axis and q -axis current
i_d^*, i_q^*	Reference stator d -axis and q -axis current
i_{cd}, i_{cq}	d -axis and q -axis iron loss current
i_{dn}, i_{qn}	Normalized stator d -axis and q -axis current
i_s	Stator current
i_{dFW}	d -axis field-weakening current
ω_e	Rotor electrical angular speed

T_e	Electromagnetic torque
T_e^*	Reference electromagnetic torque
T_{en}	Normalized electromagnetic torque
θ	Actual rotor position
θ^*	Estimated rotor position
L_d, L_q	d -axis and q -axis inductances
φ_d, φ_q	d -axis and q -axis flux linkages
φ_f	Permanent magnetic flux linkage
$\hat{\varphi}_f$	Estimated Permanent magnetic flux linkage
dL	Difference of d -axis and q -axis inductances
R_s	Stator resistance
R_c	Iron loss resistance
P_{in}	Input power
P_{out}	Output power
P_{out}^*	Reference output power
P_{loss}	Power loss
P_{Cu}	Copper power loss
V_{dc}	DC linkage voltage
T	Control period
f	Control frequency
t	Time
p	Number of pole pairs

References

- Huang, W.; Zhang, Y.; Zhang, X.; Sun, G. Accurate torque control of interior permanent magnet synchronous machine. *IEEE Tran. Energy Convers.* **2014**, *29*, 29–37. [[CrossRef](#)]
- Rostami, A.; Asaei, B. A novel method for estimating the initial rotor position of pm motors without the position sensor. *Energy Convers. Manag.* **2009**, *50*, 1879–1883. [[CrossRef](#)]
- Dong-Bin, L.U.; Ouyang, M.G.; Jing, G.U.; Jian-Qiu, L.I. Field oriented control of permanent magnet brushless hub motor in electric vehicle. *Electr. Mach. Control* **2012**, *11*, 014.
- Kim, S.Y.; Choi, C.; Lee, K.; Lee, W. An improved rotor position estimation with vector-tracking observer in pmsm drives with low-resolution hall-effect sensors. *IEEE Trans. Ind. Electron.* **2011**, *58*, 4078–4086.
- Dalala, Z.M.; Cho, Y.; Lai, J.S. Enhanced Vector Tracking Observer for Rotor Position Estimation for PMSM Drives with Low Resolution Hall-Effect Position Sensors. In Proceedings of the 2013 IEEE International Electric Machines & Drives Conference (IEMDC), Chicago, IL, USA, 12–15 May 2013; pp. 484–491.
- Lidozzi, A.; Solero, L.; Crescimbin, F.; Napoli, A.D. SVM PMSM drive with low resolution hall-effect sensors. *IEEE Tran. Power Electron.* **2007**, *22*, 282–290. [[CrossRef](#)]
- Batzel, T.D.; Lee, K.Y. Slotless permanent magnet synchronous motor operation without a high resolution rotor angle sensor. *IEEE Tran. Energy Convers.* **2001**, *15*, 366–371. [[CrossRef](#)]
- Xu, B.; Mu, F.; Shi, G.; Ji, W.; Zhu, H. State estimation of permanent magnet synchronous motor using improved square root UKF. *Energies* **2016**, *9*, 489. [[CrossRef](#)]
- Jung, S.Y.; Nam, K. Pmsm control based on edge-field hall sensor signals through anf-pll processing. *IEEE Trans. Ind. Electron.* **2011**, *58*, 5121–5129. [[CrossRef](#)]
- Boileau, T.; Leboeuf, N.; Nahid-Mobarakeh, B.; Meibody-Tabar, F. Online identification of PMSM parameters: Parameter identifiability and estimator comparative study. *IEEE Trans. Ind. Appl.* **2011**, *47*, 1944–1957. [[CrossRef](#)]
- Liu, K.; Zhu, Z.Q.; Stone, D.A. Parameter estimation for condition monitoring of PMSM stator winding and rotor permanent magnets. *IEEE Trans. Ind. Electron.* **2013**, *60*, 5902–5913. [[CrossRef](#)]
- Horen, Y.; Strajnikov, P.; Kuperman, A. Simple mechanical parameters identification of induction machine using voltage sensor only. *Energy Convers. Manag.* **2015**, *92*, 60–66. [[CrossRef](#)]
- Park, J.W.; Koo, D.H.; Kim, J.M.; Kim, H.G. Improvement of control characteristics of interior permanent magnet synchronous motor for electric vehicle. *IEEE Trans. Ind. Appl.* **2001**, *37*, 1754–1760. [[CrossRef](#)]

14. Meessen, K.J.; Thelin, P.; Soulard, J.; Lomonova, E.A. Inductance calculations of permanent-magnet synchronous machines including flux change and self- and cross-saturations. *IEEE Trans. Magn.* **2008**, *44*, 2324–2331. [[CrossRef](#)]
15. Liang, P.; Pei, Y.; Chai, F.; Zhao, K. Analytical calculation of d - and q -axis inductance for interior permanent magnet motors based on winding function theory. *Energies* **2016**, *9*, 580. [[CrossRef](#)]
16. Mohamed, Y.R.; Lee, T.K. Adaptive self-tuning MTPA vector controller for IPMSM drive system. *IEEE Trans. Energy Convers.* **2006**, *21*, 636–644. [[CrossRef](#)]
17. Urasaki, N.; Senjyu, T.; Uezato, K. An accurate modeling for permanent magnet synchronous motor drives. In Proceedings of the APEC Fifteenth IEEE Applied Power Electronics Conference and Exposition, New Orleans, LA, USA, 6–10 February 2000; Volume 381, pp. 387–392.
18. Huang, W.Q.; Zhang, Y.T.; Zhang, X.C. Research on power closed-loop torque control strategy of PMSM in HEV application. *Trans. Beijing Inst. Technol.* **2015**, *35*, 246–250.
19. Kwon, Y.C.; Kim, S.; Sul, S.K. Voltage feedback current control scheme for improved transient performance of permanent magnet synchronous machine drives. *IEEE Trans. Ind. Electron.* **2012**, *59*, 3373–3382. [[CrossRef](#)]
20. Choi, J.W.; Sul, S.K. Inverter output voltage synthesis using novel dead time compensation. *IEEE Trans. Power Electron.* **1996**, *11*, 221–227. [[CrossRef](#)]
21. Choi, J.W.; Sul, S.K. A new compensation strategy reducing voltage/current distortion in PWM VSI systems operating with low output voltages. *IEEE Trans. Ind. Appl.* **1995**, *31*, 1001–1008. [[CrossRef](#)]
22. Cheng, B.; Tesch, T.R. Torque feedforward control technique for permanent-magnet synchronous motors. *IEEE Trans. Ind. Electron.* **2010**, *57*, 969–974. [[CrossRef](#)]
23. Morimoto, S.; Sanada, M.; Takeda, Y. Wide-speed operation of interior permanent magnet synchronous motors with high-performance current regulator. *IEEE Trans. Ind. Appl.* **1994**, *30*, 920–926. [[CrossRef](#)]
24. Kim, J.M.; Sul, S.K. Speed control of interior permanent magnet synchronous motor drive for the flux weakening operation. *IEEE Trans. Ind. Appl.* **1995**, *2000*, 103–108.



© 2017 by the authors. Licensee MDPI, Basel, Switzerland. This article is an open access article distributed under the terms and conditions of the Creative Commons Attribution (CC BY) license (<http://creativecommons.org/licenses/by/4.0/>).